# Gas Evolution Dynamics in Godunov-Type Schemes

Kun Xu*
Department of Mathematics
Hong Kong University of Science and Technology
Clear Water Bay, Kowloon, Hong Kong

**subject classification:** *35L64, 76N10, 65M93, 76P05*
**key words:** *flux vector splitting and flux difference splitting*

## Abstract

As a continuous effort to understand the Godunov-type schemes, following the paper "Projection Dynamics in Godunov-Type Schemes" [29] (*Jcp Vol.142, 412-427, 1998*), in this paper we are going to study the gas evolution dynamics of the exact and approximate Riemann solvers. More specifically, the underlying dynamics of Flux Vector Splitting (FVS) and Flux Difference Splitting (FDS) schemes will be analyzed. Since the FVS scheme and the Kinetic Flux Vector Splitting (KFVS) scheme have the same physical mechanism and numerical formulations, based on the governing equation of the discretized KFVS scheme, the weakness and advantages of FVS scheme are clearly observed. Also, in this paper, the implicit equilibrium assumption in the Godunov flux will be analyzed. Due to the numerical shock thickness related to the cell size, the numerical scheme should be able to capture both equilibrium and non-equilibrium flow behavior in smooth and discontinuous regions. The Godunov flux basically lacks the mechanism to capture nonequilibrium effects in the artificially enlarged numerical shock region and to stabilize the numerical shock structure. Consequently, the Godunov method is exposed to the possible spurious solutions, such as the carbuncle phenomena and odd-even decoupling, once the dissipation provided in the projection stage is not enough.

*Email:makxu@uxmail.ust.hk Fax:(852)2358-1643 Tel: (852)2358-7433

## 1 Introduction

In the past decades, tremendous progress have been made in the development of numerical methods for compressible flow simulations. Most of them are largely based on the upwinding concepts, where the appropriate amount of numerical dissipation is implicitly included in the scheme to make the smooth shock transition possible [17, 6, 8]. In the earlier paper, we have analyzed the projection dynamics in the Godunov method[29], where the implicit viscous effect is qualitatively obtained. As a continuous effort to understand the Godunov method, in this paper we are going to analyze the dynamics in the gas evolution stage, *i.e.* the physics in the exact and approximate Riemann solvers.

There are mainly two kinds of flux functions used for the inviscid Euler equations. The first group is the FVS schemes [23, 25], where the waves generated in the left and right hand sides of a cell interface move across the cell interface freely. The ignorance of dynamical wave interactions between the left and right moving waves in the FVS scheme is basically inappropriate. For example, it is physically unreasonable to observe that in the FVS scheme a right moving wave from the left state can evolve through the cell interface regardless of the right state. Since both the dynamical model and the flux formulation of the FVS scheme of van Leer is identical to the Kinetic Flux Vector Splitting (KFVS) scheme based on the collisionless Boltzmann equation [8, 15], in this paper, the governing equation for the KFVS scheme will be derived, from which the numerical dissipation in the scheme can be clearly observed. For example, the over-diffusivity for the Navier-Stokes shear layer calculations can be well explained [23, 26]. Also, many misunderstanding about the equivalence between the collisionless Boltzmann equation and the Euler equations will be clarified[21, 15, 19].

In contrast, the exact Riemann solver and the FDS scheme account for the wave interactions in the gas evolution process across a cell interface [6, 22, 18]. This kind of interaction can be clearly observed in the Roe's approximate Riemann solver, where Roe's average is actually a constructed correlation of the flow variables between two constant states. Since the FDS scheme is more closely to solve the inviscid Euler equations, the physical viscous term in the Navier-Stokes simulation will not be poisoned by the numerical viscosities generated in the FDS scheme. For example, the Roe's Riemann solver and other FDS methods can precisely keep a shear layer in the 2D case once the shear layer is aligned with the mesh. However, this advantage is also accompanied with disadvantage. Physically, the fluid inside a numerical shock layer stays in a highly non-equilibrium state and dissipation is extremely important to translate kinetic energy into thermal energy and stablize the shock structure. However, the Godunov method ignores the non-equilibrium fact even inside the numerical shock region, and the flux function is solely based on the equilibrium assumption. The inappropriate use of equilibrium state leads to spurious solutions, such as carbuncle phenomena and odd-even decoupling [20]. On the other hand, the FVS schemes do not generate these spurious solutions, since they are intrinsically solving "viscous" equations rather than the inviscid Euler equations. So, an optimum choice to get a better scheme is to combine both the FVS and FDS methodology, to develop the so-called hybrid schemes [3, 4, 10, 13, 16, 2]. The detail explanation will be presented in this paper.

In this paper, section 2 is about the physical analysis of the FVS scheme, and section 3 is related to the FDS scheme. Section 4 gives reasons for the necessity of developing hybrid schemes, which combines both the FVS and FDS methods. The last section is the conclusion and future perspective in the development of numerical methods for compressible flow simulations.

## 2 Flux Vector Splitting Scheme

Flux vector splitting is a technique for achieving upwind bias in numerical flux function, which is a natural consequence of regarding a fluid as an ensemble of particles. Since particles can move forward or backward, this automatically splits the fluxes of mass, momentum and energy into forward and backward fluxes through the cell interface, *i.e.*

$$F_{j+1/2} = F^{+}(W_j) + F^{-}(W_{j+1}),$$

where $W_j$ represents mass, momentum and energy densities inside cell $j$. The equivalence between the above splitting mechanism and the collisionless Boltzmann equation was first realized by Harten, Lax and van Leer [8]. Numerically, it is observed that the explicit flux formulation of the Kinetic Flux Vector Splitting (KFVS) scheme by solving the collisionless Boltzmann equation is identical to the flux function of van Leer [15]. In order to understand the FVS scheme, in the following we are going to have a detail analysis of KFVS scheme and derive the governing equation for the discretized scheme. All conclusion can be equally applied to the general FVS schemes[23, 25].

It is well-known that the Euler equations can be derived from the Boltzmann equation with the local equilibrium distribution function. For an equilibrium state, $f$ is equal to the Maxwellian distribution $g$, the collision term $Q(f,f)$ goes to zero automatically, *i.e.* $Q(g,g) \equiv 0$. So, in this case, the Boltzmann equation in 1-D case becomes

$$f_t + u f_x = 0. \tag{2.1}$$

Since there is no collision term on the right hand side of the above equation, this equation is also called the collisionless Boltzmann equation. The KFVS scheme based on the above equation and using the Maxwellian distribution function as the equilibrium state inside each cell was first proposed by Pullin [21], and his scheme was named Equilibrium Flux Method (EFM) instead of KFVS. With the initial condition of the gas distribution function $f_0(x,0)$, the exact solution of the collisionless Boltzmann equation is

$$f = f_0(x - ut, t). \tag{2.2}$$

For example, for the same initial condition as the Riemann problem, two constant equilibrium states at $x \leq 0$ and $x > 0$ can be constructed,

$$
\begin{aligned}
f_0 &= \begin{cases} g_l, & x \leq 0 \\ g_r, & x > 0 \end{cases} \\
&= g_l(1 - \mathrm{H}(x)) + g_r \mathrm{H}(x),
\end{aligned} \tag{2.3}
$$

where $\mathrm{H}(x)$ is the Heaviscid function. Note that the equilibrium states $g_l$ and $g_r$ have a one to one correspondence with the macroscopic flow variables. For example, the equilibrium Maxwellian $g$ has the form in 1-D case,

$$
g = \rho(\frac{\lambda}{\pi})^{K+1} e^{-\lambda((u-U)^2+\xi^2)}, \tag{2.4}
$$

where the parameters $(\rho, U, \lambda)$ are related to the macroscopic mass, momentum and energy densities $(\rho, \rho U, \rho\epsilon)$ through the relation

$$
\rho = \rho, \quad U = U, \quad \lambda = \frac{K+1}{4} \frac{\rho}{\rho\epsilon - \frac{1}{2}\rho U^2}. \tag{2.5}
$$

The parameter $K$ is the dimension of internal variable $\xi$ which is related to the specific heat ratio $\gamma$ [28]. From the initial condition in Eq.(2.3), the exact solution from the collisionless Boltzmann equation becomes

$$
f(x,t) = f_0(x - ut) = g_l(1 - \mathrm{H}(x - ut)) + g_r \mathrm{H}(x - ut). \tag{2.6}
$$

Since $t > 0$, the above equation can be reformulated as

$$
\begin{aligned}
f(x,t) &= g_l(1 - \mathrm{H}(\frac{x}{t} - u)) + g_r \mathrm{H}(\frac{x}{t} - u) \\
&= f(\frac{x}{t}),
\end{aligned} \tag{2.7}
$$

which is a similarity solution! So, similar to the Riemann solution of the Euler equations, the collisionless Boltzmann equation also provides a similarity solution for the case with two constant initial states. As an example, the similarity density distributions from the exact Riemann solver and the collisionless Boltzmann equation are shown in Fig.(1), where both curves have the same initial condition

$$
(\rho, U, p) = \begin{cases} (1.0, 0.0, 1.0), & x \leq 0 \\ (0.1, 0.0, 0.1), & x > 0 \end{cases}. \tag{2.8}
$$

From this figure, it is clear that the collisionless Boltzmann equation provides a smooth transition between left and right states, rather than developing distinguishable waves as that in the Euler solutions. Physically, the two curves in Fig.(1) are two limits with the collision time $\tau = \infty$ (collisionless Boltzmann) and $\tau = 0$ (Euler).

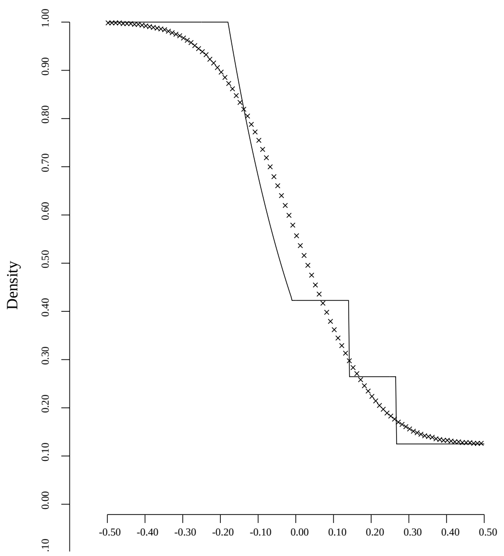


Figure 1: Density distribution from exact Euler (solid line) and collisionless Boltzmann (× symbol) solutions

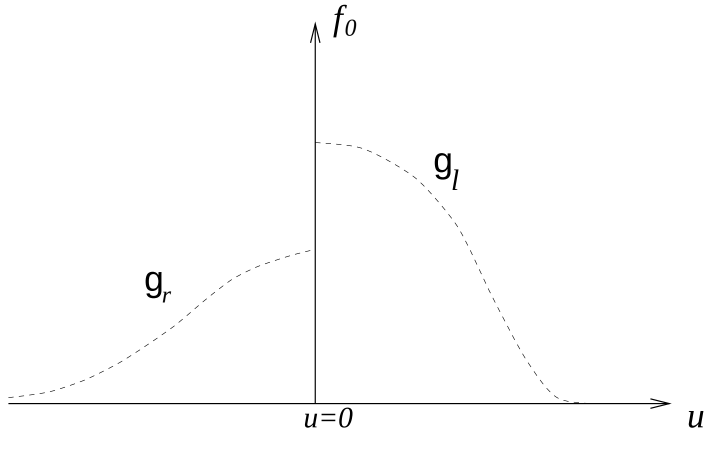


Figure 2: Gas distribution function at a cell interface for flux evaluation

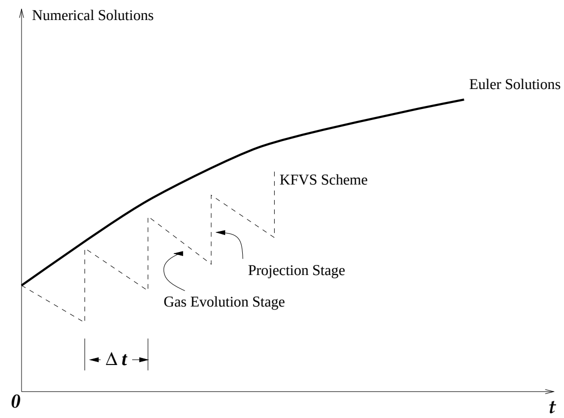


Figure 3: KFVS solution vs Euler solution, where $\Delta t$ is the CFL time step.

It is true that *if* the flow remains in a local equilibrium state, Eq.(2.1) is the correct description of the Euler equations. However, even with initial equilibrium states, the collisionless Boltzmann equation cannot keep the equilibrium state dynamically. More specifically, the evaluation of flux function in KFVS scheme is actually based on two half Maxwellians at a cell interface instead of using a single equilibrium state. Look at the solution $f$ at $x = 0$ and $t > 0$ in Eq.(2.7) and Fig.(2). Physically, the mechanism for bringing the distribution function close to the equilibrium state is the collisions suffered by the molecules of the gas, the so-called collision term in the Boltzmann equation. But, the collisionless Boltzmann equation in the gas evolution stage totally ignores this dynamical process.

Although the KFVS scheme lacks particle collisions in the gas evolution stage, numerically it still can be used in the compressible flow calculations, and the numerical solution is different from free particle stream solutions. The basic reason for this is that an artificial collision term has been implicitly added in the projection stage in the KFVS method. For example, at the end of each time step, a Maxwellian distribution function inside each cell is re-initiated, which is equivalent to bringing particle collisions instantaneously to make the transition from the non-equilibrium state $f$ to equilibrium state $g$ inside each cell. Therefore, in the gas evolution stage, the KFVS scheme solves the collisionless Boltzmann equation

$$\frac{\partial f}{\partial t} + u\frac{\partial f}{\partial x} = 0. \tag{2.9}$$

In the projection stage, it solves

$$\frac{\partial f}{\partial t} = Q(f, f), \tag{2.10}$$

where an equilibrium Maxwellian distribution is constructed inside each cell using the conserved mass, momentum and energy. If we combine the gas evolution and projection stages, the real governing equation of the KFVS scheme is the following modified "BGK" model,

$$\frac{\partial f}{\partial t} + u\frac{\partial f}{\partial x} = \frac{g - f}{\Delta t}, \tag{2.11}$$

where the real particle collision time $\tau$ in BGK model is replaced by the numerical time step $\Delta t$. The dynamical effect from the two numerical stages in the KFVS scheme is qualitatively described in Fig.(3), where the free transport in the gas evolution stage evolves the system away from the Euler solution ($f$ becomes more and more different from a Maxwellian), the projection stage drives the system towards to the Euler solutions (the instantaneous preparation of equilibrium states).

Once we have Eq.(2.11), all theoretical results related to the BGK model of the approximate Boltzmann equation can be applied [1]. The first and direct consequence is that KFVS satisfies the entropy condition[12]. Numerically, the entropy-violating solutions have never been observed in the KFVS scheme. Also, the positivity property can be obtained[5], and the scheme can be used to study any high Mach number flow passing an object, such as $M = 10^4$, without generating negative density and pressure. The modified BGK model gives the intrinsic viscosity coefficient $\eta$ and heat conductivity coefficient $\kappa$ in the KFVS scheme,

$$\eta = p\Delta t, \tag{2.12}$$

and

$$\kappa = \frac{K+5}{2}\frac{k}{m}p\Delta t, \tag{2.13}$$

where $p$ is the pressure, $k$ the Boltzmann constant, and $m$ the molecule mass. So, the KFVS scheme is solving the "Navier-Stokes" equations and the viscosity and heat-conductivity coefficients are proportional to the time step. Applying the KFVS/EFM method of Pullin to the shear layer directly, similar dissipative coefficients have been obtained in [14]. In the KFVS scheme, the free particle transport inside each time step brings the practical particle mean free path equal to the cell size. Physically, this is the main reason for the robustness of the KFVS scheme, because the numerical shock thickness ($\sim \Delta x$) requires that the numerical mean free path is on the order of cell size. Therefore, the numerical dissipative coefficients are proportional to the cell size or time step in the shock region. As a result, the KFVS scheme totally avoids the carbuncle phenomena and odd-even decoupling [7]. Although the artificial collisions make the KFVS scheme extremely robust and provide a most reasonable mechanism to construct the numerical shocks, the large artificial dissipation also poisons the Navier-Stokes solutions, such as the shear and boundary layer calculations[13, 26].

The over-diffusivity in the KFVS scheme is closely related to the splitting of the Boltzmann equation into Eq.(2.9) and (2.10). In order to improve the kinetic scheme, the gas-kinetic BGK method solves the Boltzmann equation without splitting the advection and collisions terms in the gas evolution stage, where

$$\frac{\partial f}{\partial t} + u\frac{\partial f}{\partial x} = \frac{g-f}{\tau}$$

is solved for the flux function directly. As a result, the gas-kinetic BGK method couples the viscosity and heat conductivity coefficients to the particle collision time $\tau$, instead of the time step $\Delta t$. So, accurate Navier-Stokes solutions can be captured by the BGK method by appropriately choosing the collision time $\tau$ according to the physical viscosity coefficient[28].

## 3 Flux Difference Splitting Scheme

The main purpose of this section is to examine the dynamical effect in the exact Riemann solver and the FDS scheme. At the same time, spurious solutions from the Riemann solver, *i.e.* the odd-even decoupling and carbuncle phenomena in the 2D case, are well explained.

The Riemann problem is defined as an Initial Value Problem for the Euler equations in the 1-D case. With the following initial condition at $t = 0$,

$$(\rho, U, p)(x, 0) = \begin{cases} (\rho_L, U_L, p_L), & x < 0, \\ (\rho_R, U_R, p_R), & x > 0, \end{cases} \tag{3.14}$$

the entropy-satisfying solutions are the following: the left state $(\rho_L, U_L, p_L)$ is connected to the right state $(\rho_R, U_R, p_R)$ by a 1-shock or 1-rarefaction wave, a 2-contact discontinuity, and a 3-shock or a 3-rarefaction wave. The 2-contact discontinuity separates two constant states $(\rho_I, U^*, p^*)$ and $(\rho_{II}, U^*, p^*)$ so that $(U, p)$ are continuous across the contact discontinuity. For example, in Fig.(4), the 1-wave is a rarefaction and the 3-wave a shock. There is standard technique to obtain the solutions around a contact discontinuity [24].

Once the solution for the Riemann problem is obtained, the values at $x = 0$, *e.g.* $(\rho_I, U^*, p^*)$ in Fig.(4), can be used to construct fluxes. The Godunov method uses these fluxes across each cell interface to update the flow variables inside each cell. In order to understand the Godunov method, we have to figure out the underlying assumption in the process of evaluating fluxes. For the Euler equations, it is obvious that once we know $(\rho, U, p)$, the corresponding fluxes are

$$\begin{pmatrix} F_\rho \\ F_{\rho U} \\ F_{\rho\epsilon} \end{pmatrix} = \begin{pmatrix} \rho U \\ \rho U^2 + p \\ \frac{1}{2}\rho U^3 + \frac{\gamma}{\gamma-1} pU \end{pmatrix}. \tag{3.15}$$

For example, in Fig.(4), the fluxes at $x = 0$ are $(\rho_I U^*, \rho_I U^{*2} + p^*, \frac{1}{2}\rho_I U^{*3} + \frac{\gamma}{\gamma-1} p^* U^*)^T$. From the flow variables $(\rho, U, p)$ to the flux functions $(F_\rho, F_{\rho U}, F_{\rho\epsilon})$, it is implicitly assumed that the gas is staying

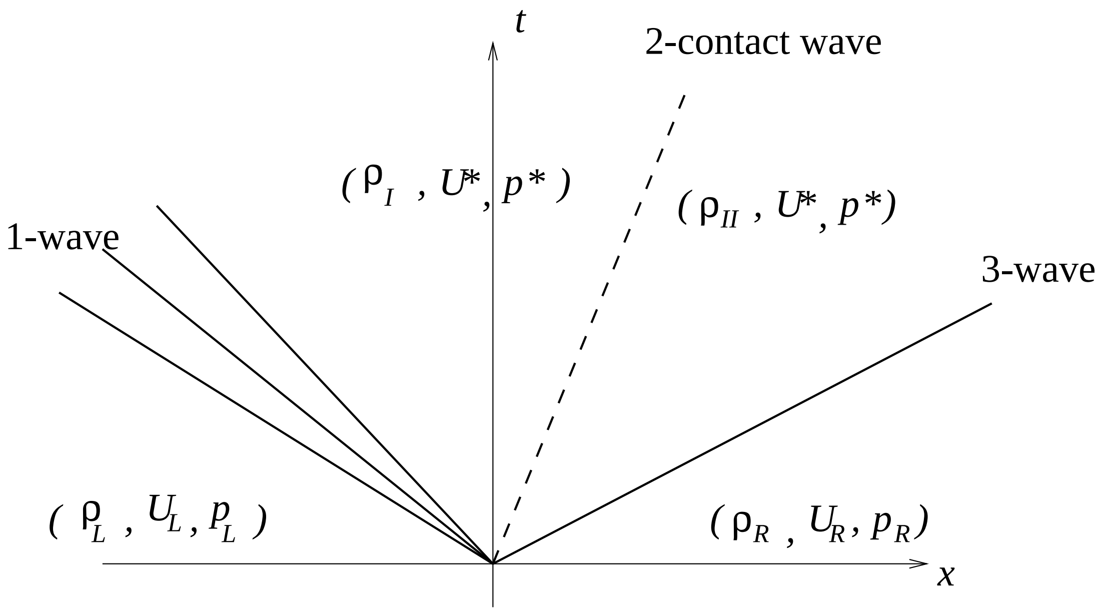


Figure 4: Solution of the Riemann Problem in the $(x, t)$-Plane

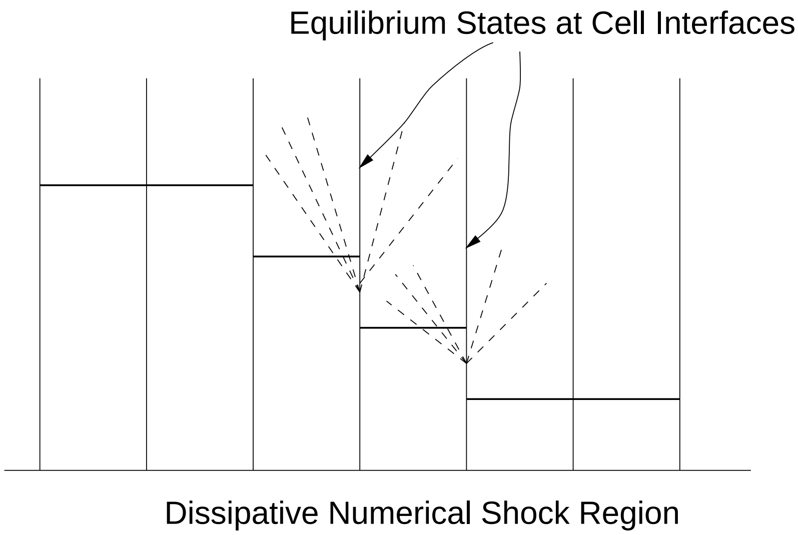


Figure 5: Godunov Gas Evolution Model

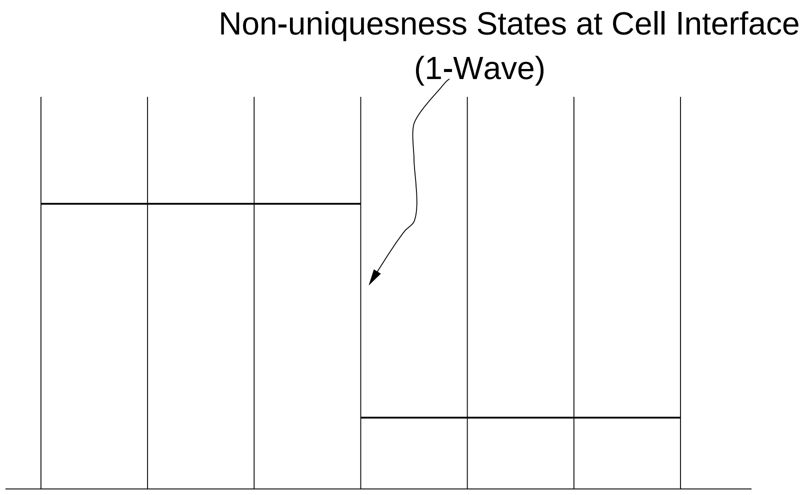


Figure 6: A stationary shock front located exactly at a cell interface

in an equilibrium state. In other words, whatever the real flow situations is, the state $(\rho_I, U^*, p^*)$ at the cell interface always corresponds to a Maxwellian distribution function in Godunov method, even for the fluid inside a numerical shock layer, see Fig.(5). As we know, the intermediate points in the numerical shock region have to be regarded as points inside a shock structure, where the dissipative mechanism is crucially important to translate kinetic energy into thermal energy and make the smooth numerical shock transition. However, the gas evolution model of the Godunov flux mis-interprets this region as a nondissipative flow region and assigns the equilibrium state there. In the special case, if the shock is located exactly at a cell interface, the Godunov method can capture a stationary shock exactly, such as that shown in Fig.(6). However, if we look at the Riemann solution in this case, we cannot even find an unique state $(\rho, U, p)$ at the cell interface. So, in this case the Godunov method uses the continuous fluxes directly, which avoids constructing any equilibrium state, consequently avoids any error. In the general case, once the numerical shock covers a few grid points, the weakness of the Godunov method emerges. Ignoring of nonequilibrium property in the shock region in 1-D case is not harmful because the artificial dissipation is provided anyway in the projection stage[29], however in 2D case, it is one of the direct reasons for the happening of carbuncle phenomena and odd-even decoupling in the Godunov method.

In the 1-D case, there is always projection dissipation to support a numerical shock structure. However, in the 2-D case, if the shock front is aligned with the numerical mesh, the projection dissipation could mainly be provided in the direction normal to the shock front. Along the shock

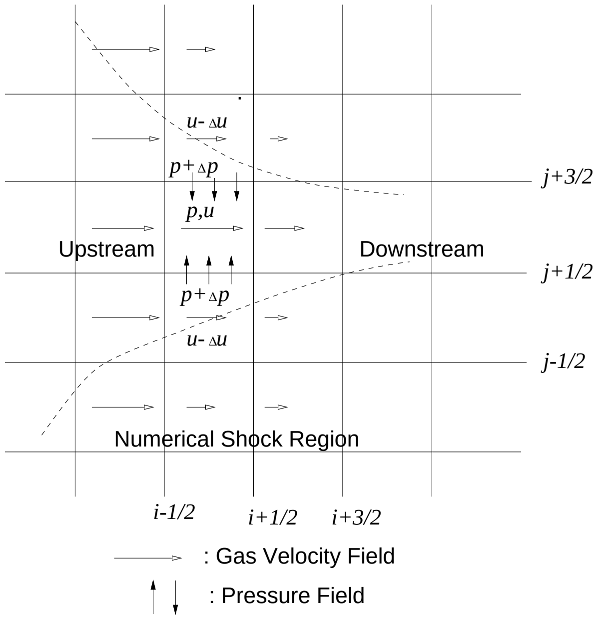


Figure 7: Schematic explanation of shock instability

front the Godunov method solely observes an uniform flow, or a shear flow if there is perturbation in the velocity field. In order to have the carbuncle phenomena or odd-even decoupling to happen, the numerical flow has to satisfy the following conditions [20, 11];
(1). Shock propagates and is aligned with the mesh[1].
(2). The mass flux due to a pressure difference is not zero, such as $D^{(p)} \neq 0$ in the dissipative term $\mathcal{D} = \mathcal{D}^{(\rho)}\Delta\rho + \mathcal{D}^{(U)}\Delta U + \mathcal{D}^{(p)}\Delta p$ of the full flux function $F_{j+1/2} = \frac{1}{2}(F_j + F_{j+1}) + \mathcal{D}$.
From point (1), if the shock is aligned with the mesh, the projection dissipation is only provided in one direction, such as $x$-direction in Fig.(7), and there is almost no projection dissipation provided in the $y$-direction along the shock front. Note that the projection dissipation is proportional to the square of velocity differences $(\mathbf{U}_1 - \mathbf{U}_2)^2$ [29].

Now suppose that a numerical shock is propagating in the $x$-direction as shown in Fig.(7). Due to numerical perturbations, it is possible for certain cells (not necessarily to be one cell !) to have slight larger velocity and less pressure, or the opposite[2]. Once this kind of perturbation exist at the numerical shock front, such that the increase in velocity and decrease in pressure in central cells in

[1]Small misalignments are necessary for the shock perturbations.

[2]For example, when flow passing 1-D nozzle with variable cross section, the change of velocity $\Delta U$ is always opposite to the change of pressure $\Delta p$.

Fig.(7), physically the shear viscosity will strongly take effect to reduce the velocity differences and stablize the numerical shock front. However, numerically, solving the inviscid Euler equations in $y$-direction will give a different answer. The exact 1-D Riemann solver in $y$-direction does not recognize the slight $x$-component velocity differences due to the inviscid nature. The only dynamical effect involved in the Riemann solver in this direction is the pressure difference. Since the surrounding cells have a higher pressure, they will push the fluid towards center. As a consequence, the fluid in central cells passes through an even narrower region. According to the Bernoulli equation, the fluid speed will get even higher due to the converging of streamlines. As a result, the pressure in central cells is even lower. So, the Euler fluxes or the exact Riemann solver in $y$-direction could only help to amplify the initial perturbations, and the numerical fluid will speed up and penetrate the shock layer to form instabilities. We can also understand the above picture in an easier way. In the $y$-direction, since the inviscid Euler equations are solved. It corresponds to a perturbed shear layer with $Re = \infty$. So, generating instability is not surprising at all.

The above explanation validates Liou's conjecture that $\mathcal{D}^{(p)} \neq 0$ is accompanied by an instability [11]. If $\mathcal{D}^{(p)} = 0$, the initial pressure difference in $y$-direction will not push the fluid towards the central cells, and no instability will be formed. Unfortunately, even for the exact Riemann solver, $\mathcal{D}^{(p)} \neq 0$ always holds. So, the carbuncle phenomena or odd-even decoupling are intrinsically rooted in the Godunov method if there is enough perturbation in the shock region and the shock is aligned with the mesh. The above explanation has no conflict with the stability of inviscid shock [9], where a discontinuity shock (without structure) is perturbed and is stable. Here, in our analysis, we are concerning with the stability of numerical shock structure, where the dynamics of constructing shock is more important.

In conclusion, the odd-even decoupling (perturbation from moving shock) and carbuncle phenomena (perturbation from slightly irregular mesh) are due to the numerical discretization of the inviscid Euler equations. Conditions (1) and (2) are necessary to have this kind of phenomena to take place. In order to stabilize the shock front in $y$-direction, a direct way is to add dissipation through entropy fix. However, as realized by Quirk[20], the entropy fix here is added in the shear layer rather than in the shocks[3]. So, solving the viscous equations becomes necessary, not only to get entropy-satisfying shock solution, but also to stabilize the possible shear layer.

## 4 Hybrid Schemes

The flux functions for the FVS and FDS schemes are usually written as

$$F_{j+1/2} = \frac{1}{2}(F_j + F_{j+1}) + \mathcal{D}_{j+1/2},$$

[3] The $y$-direction Riemann solver does not know that there is a shock in the $x$-direction.

where $\mathcal{D}_{j+1/2}$ is the dissipative flux. Basically, this expression is not very precise. The real distinguishable point between viscous and inviscid flux should be related to whether the flux function can be obtained from equilibrium state or not. For the FVS flux, the dissipative character can be clearly seen from the two half Maxwellians. However, for the Godunov method, the flux function is actually related to a single Maxwellian, which only provides inviscid flux. The dissipation needed for the shock transition in Godunov method is from the projection stage rather than the flux function itself[29].

The weakness of the Godunov method results from the equilibrium representation of fluid regardless of the real physical situation. The ability to capture a stable discontinuous solution for FDS scheme in the multidimensional case is rather fragile, especially in cases where high resolution calculation on a fine mesh is required. So, spurious solutions are occasionally observed for the Godunov method. However, for the numerical solution in smooth regions, such as boundary layer solutions of the Navier-Stokes equations, the absence of dissipation in the Riemann solver becomes an advantage, where the boundary solutions can be obtained accurately.

On the other hand, for the FVS scheme, the governing equation in the gas evolution stage is the collisionless Boltzmann equation. The free transport in the gas evolution stage, along with the projection dissipation, naturally introduces large dissipation. Although the large dissipation due to the nonequilibrium property could help the scheme to be extremely robust, the contact discontinuities and slip lines are badly smeared. As a consequence, the Navier-Stokes solutions cannot be properly represented by FVS schemes [26, 13], especially with coarse mesh ($\eta \sim \Delta x$).

In order to construct a scheme with both robustness and accuracy, a recent trend in the development of upwind schemes has centered around the construction of hybrid flux-splitting formulations which combines the accuracy of FDS approach in the resolution of shear layers with the robustness of FVS method in the capturing of strong discontinuities. For example, starting from the FVS scheme, in order to reduce the free penetration of different waves or particles, the correlation or collisions between left and right moving waves have to be introduced. The construction of the common $M_{1/2}, U_{1/2}$ terms in AUSM-type schemes is largely based on this physical consideration[10]. Similarly, Moschetta and Pullin [16] tried to use Osher's numerical flux to replace linearly degenerate wave in the KFVS scheme. From the FDS scheme, additional dissipations are usually introduced to stabilize discontinuous solutions [27]. The main dynamical effects of using two waves instead of three waves in the HLL scheme is to smear some waves and introduce dissipations [8]. Similar philosophy can be observed in Marquina's flux function [3], where Steger and Warming's FVS flux is modified. A good hybrid scheme depends on a smart weight function to identify where the flow is smooth or where the flow is discontinuous. It is difficult to rationalize the most constructions of hybrid splitting schemes on a rigorous physical basis. The questionable point for these hybrid methods is that they are not based on any rigorous governing equations, rather than *ad hoc* fixes for any mistakes in the old approach. Also, no uniform criteria have ever been established so far for the optimum choice. Numerically, as tested by Gressier and Moschetta [7], almost no hybrid schemes [11, 2, 16] could really remove the pathological behavior of upwind schemes in the refining mesh study. A possible way to avoid the above uncertainties in the designing of robust and accurate scheme is to construct a viscous governing equation or to solve the existing viscous equations. The BGK method is an example in this aspect, it naturally provides a genuine nonlinear combination of the FVS and FDS schemes, and this combination is based on the physical BGK model, where the collision time $\tau$ is related to the physical viscosity in smooth region and to the amplified artificial viscosity in the discontinuity region [28].

## 5 Conclusion

Quite often, the requirements for robustness and accuracy in the design of a numerical scheme are in conflict with each other: if a scheme is robust, it is unnecessarily diffusive; if a scheme is accurate, it loses robustness. In order to get a correct representation of flow motion in the discretized space and time, a consistent dissipative mechanism must be added in the gas evolution stage, and it should be based on the correct governing equation.

It seems that the inviscid Euler equations cannot give a correct representation for the "numerical" fluid. Due to the limited cell size and time step, an appropriate viscous equations have to be solved directly. It is very difficult to find any perfect Riemann solver if only the Euler equations are regarded as the target equations for the numerical fluid. Also, it is unlikely that any hybrid scheme will become very successful if there is no any explicit governing equations in the designing of such a scheme. Basically, all attempts to obtain hybrid schemes are processes of solving new modified governing equations under discretized schemes.

## Acknowledgments

The current research is supported by the Research Grant Council of Hong Kong through RGC Competitive Earmarked Research Grant HKUST6166/97P.

## References

[1] P.L. Bhatnagar, E.P. Gross, and M. Krook (1954), "A Model for Collision Processes in Gases I: Small Amplitude Processes in Charged and Neutral One-Component Systems", *Phys. Rev.* , **94**, 511-525.

[2] F. Coquel and M.S. Liou (1995), "Hybrid Upwind Splitting (HUS) by a Field by Field Decomposition", NASA TM-106843.

[3] R. Donat and A. Marquina (1996), "Capturing Shock Reflections: An Improved Flux Formula", *J. Comput. Phys.*, Vol.125, 42-58.

[4] J.R. Edwards (1997), "A Low-Diffusion Flux-Splitting Scheme for Navier-Stokes Calculations", *Computers & Fluids*, Vol.26, No.6, 635-659.

[5] E. Godlewski and P.A. Raviart (1996), "Numerical Approximation of Hyperbolic Systems of Conservation Laws", Springer.

[6] S.K. Godunov (1959), " A Difference Scheme for Numerical Computation of Discontinuous Solutions of Hydrodynamic Equations", Math. Sbornik, **47**, 271.

[7] J. Gressier and J.M. Moschetta (1998), "On the Pathological Behavior of Upwind Schemes", AIAA 98-0110.

[8] A. Harten, P. D. Lax, and B. Van Leer (1983), "Upstream differencing and Godunov-type schemes for hyperbolic conservation laws," *SIAM Rev.* Vol.25.

[9] L.D. Landau and E.M. Lifshitz (1987), "Fluid Mechanics", Pergamon Press.

[10] M.S. Liou and C.J Steffen (1993), "A New Flux Splitting Scheme", *J. Comput. Phys.*, Vol.107, 23.

[11] M.S. Liou (1997), "Probing Numerical Fluxes, Positivity, and Entropy-satisfying Property", AIAA 97-2035 (unpublished).

[12] S.H. Lui and K. Xu (1998), "Entropy Analysis of Gas-Kinetic Schemes for the Compressible Euler Equations", submitted to *SIAM J. Numer. Anal.*.

[13] R.W. MacCormack and G.V. Candler "The solution of the Navier-Stokes equations using Gauss-Seidel Line Relaxation", Computer & Fluids, Vol.17, No.1, P135, 1989.

[14] M.N. Macrossan (1989), "The Equilibrium Flux Method for the Calculation of Flows with Non-Equilibrium Chemical Reactions", J. of Comput. Phys. **80**, 204-231.

[15] J. C. Mandal and S.M. Deshpande (1994), "Kinetic Flux Vector Splitting for Euler Equations", Computers and Fluids, **23** , No.2, 447.

[16] J.M. Moschetta and D. Pullin (1997), "A Robust Low Diffusive Kinetic Scheme for the Navier-Stokes/Euler Equations", J. Comput. Phys., Vol.133, 193-204.

[17] J.V. Neumann and R.D. Richtmyer (1950), *J. Appl. Phys.*, Vol.21, 232.

[18] S. Osher and F. Solomon (1982), "Upwind Difference Schemes for Hyperbolic Systems of Conservation Laws", *Math. Comput.*, **38**, 339-374.

[19] B. Perthame (1992), "Second-order Boltzmann Schemes for Compressible Euler Equations in One and Two Space Dimensions", *SIAM J. Numer. Anal.*, **29**, No.1.

[20] Quirk, J. (1994), "A Contribution to the Great Riemann Solver Debate", Int. J. Num. Met. in Fluids, **18**, no.6.

[21] Pullin, D.I. (1980), "Direct Simulation Methods for Compressible Inviscid Ideal Gas Flow", J. of Comput. Phys. **34**, 231-244.

[22] P.L. Roe (1981), "Approximate Riemann Solvers, Parameter Vectors and Difference Schemes", J. Comput. Phys., **43**, 357.

[23] J. L. Steger and R. F. Warming, "Flux vector splitting of the inviscid gas-dynamic equations with applications to finite difference methods", J. Comput. Phys., 40, 263-293 (1981).

[24] E. Toro (1997), "Riemann Solvers and Numerical Methods for Fluid Dynamics", Springer.

[25] B. van. Leer , "Flux-Vector Splitting for the Euler Equations", ICASE report, NO.82-30, September, 1982.

[26] B. van. Leer , J.L. Thomas, P.L. Roe and R.W. Newsome, "A Comparison of Numerical Flux Formulas for the Euler and Navier-Stokes Equations", AIAA paper 87-1104, 1987.

[27] Woodward, P. and Colella, P. (1984), "Numerical Simulations of Two-dimensional Fluid Flow with Strong Shocks", J. Comput. Phys. **54**, 115.

[28] K. Xu (1998), "Gas-Kinetic Schemes for Unsteady Compressible Flow Simulations", VKI for Fluid Dynamics Lecture Series 1998-03, Computational Fluid Dynamics.

[29] K. Xu and J. Hu (1998) "Projection Dynamics in Godunov-type Schemes", *J. Comput. Phys.*, **142**,412-427.